THE ASTROPHYSICAL JOURNAL, 329:82–96, 1988 June 1

MEASUREMENTS OF THE GAS TEMPERATURE AND IRON ABUNDANCE DISTRIBUTION IN THE COMA CLUSTER

JOHN P. HUGHES, P. GORENSTEIN, AND D. FABRICANT
Harvard-Smithsonian Center for Astrophysics
Received 1987 September 8; accepted 1987 November 11

ABSTRACT

The medium energy X-ray detectors onboard the *EXOSAT Observatory* have been used to determine the gas temperature at several positions in the Coma Cluster of galaxies. We find evidence at greater than 95% confidence for a higher temperature in the center of the cluster than in a position approximately 45′ off-center. No difference in iron abundance is observed between the center and off-center regions and the equilibrium model for the distribution of elements in the Coma Cluster of Abramopoulos, Chanan, and Ku can be rejected with greater than 99.5% confidence, in favor of a model with more uniform composition. We offer a phenomenological model of the Coma Cluster, which is consistent with the data presented here, as well as the imaging data from the *Einstein Observatory* and the *Tenma* X-ray spectrum. The model has a central isothermal region of temperature ~9 keV extending to ~25′ (~1 Mpc). Beyond this radius the temperature falls as a polytrope with index ~1.6.

Subject headings: galaxies: clustering — galaxies: intergalactic medium — X-rays: sources

I. INTRODUCTION

X-ray studies of the morphology and density distribution of the hot gas in clusters of galaxies have progressed significantly with the use of the imaging instruments onboard the *Einstein Observatory* and *EXOSAT*. However, progress in understanding the temperature distribution of the gas has been much slower, since imaging instruments to date have lacked efficiency at energies needed to measure cluster temperatures ($kT \sim 7$–10 keV). Yet knowledge of the temperature distribution is crucial for reconstructing the thermal history of the gas and estimating the distribution of dark matter.

Most recent attempts to determine the temperature distribution of the gas in clusters of galaxies have been based upon integrated X-ray spectrum from the entire cluster. The Coma Cluster, for example, has been observed by instruments such as *HEAO 1* A-2 (Henriksen and Mushotzky 1986) and *Tenma* (Okumura *et al.* 1988), with fields of view on the order of several degrees. In the analysis of such data, models for the temperature distribution are fitted to the integrated spectra, and limits on the model parameters (e.g., polytropic indices) are determined. These techniques suggest that the gas is not isothermal, although background subtraction and detector gain variations complicate the analysis. In addition, models of the temperature distribution may not be adequate. Integrated spectra cannot distinguish between a global spatial variation in temperature and a model with a number of local regions with different temperatures. Furthermore, if the distribution is a global radial variation, it is not possible to determine the sign of the temperature gradient.

This paper describes the results of an observation to determine the radial temperature variation in the Coma Cluster. The cluster was observed at its center and at several positions 45′ away with the medium energy proportional counters (ME) onboard the *EXOSAT Observatory*. These detectors were sensitive to X-rays in the band 2–10 keV, well-matched to the Coma Cluster which has an average kT of about 7.5 keV. The ME field of view was well-collimated with a FWHM of 45′. The energy resolution of the detectors was sufficient (21% at 6 keV) to allow determination of the cluster iron abundance from the K_α iron line complex at about 6.7 keV.

Recently similar projects have been carried out for the Virgo (Edge, Stewart, and Smith 1987; Smith and Stewart 1985) and Perseus Clusters (Ulmer *et al.* 1987). Virgo was observed with the *EXOSAT* ME detectors and was found to have a nearly constant temperature distribution ($kT \sim 2.6$ keV) over radii from 10′ to 100′ (44 kpc to 440 kpc). Ulmer *et al.* (1987) found that kT in Perseus varied from 3.6 keV at the center to 6.1 keV in an off-center region extending from 6′ to 20′ (190 kpc to 600 kpc for $H_0 = 50$ km s^{-1} Mpc^{-1}). Both of these clusters contain several complex components in addition to the smooth cluster X-ray emission. The X-ray emission from Virgo is roughly centered on the giant elliptical galaxy M87, which seems to be associated with a cooling flow (Fabian, Nulsen, and Canizares 1984). The Perseus Cluster contains several components associated with NGC 1275: a point source with a power-law X-ray spectrum, as well as a cooling flow. This latter component is what gives rise to the positive temperature gradient. By contrast, the Coma Cluster is much simpler, with no central point sources in the X-ray images, or apparent cooling flows. In addition our temperature and iron abundance constraints come from a somewhat larger region than the two clusters above. The effective average cluster radii (weighted by surface brightness and collimator response) sampled by our observations were 11′ for the center pointing and ~22′ for the off-center ones. At the Coma Cluster distance of ~140 Mpc, these radii correspond to about 450 and 900 kpc, respectively.

We address the following results on the Coma Cluster: (*a*) the *EXOSAT* measurements of temperature and iron abundance in a 45′ × 45′ central region and three similar size regions displaced 45′ east, west, and south of the center, (*b*) the relative integrated surface brightness of these regions in the 2–10 keV band, (*c*) the temperature and iron abundance of a ~3° region centered on Coma observed by *Tenma*, and (*d*) the surface brightness distribution in the 0.5–4 keV band observed

by the *Einstein Observatory*. Results (*a*) and (*b*) are new measurements described in this paper; (*c*) and (*d*) have been published elsewhere (Hughes *et al.* 1988).

The following section (§ II) presents a discussion of the data reduction and analysis procedure for the *EXOSAT* observations. We have paid particular attention to systematic errors arising from background subtraction and the determination of the detector gain. Values for the radial variation of temperature and iron abundance are derived. In § III comparison is made to several models for the surface brightness distribution, the radial variation in temperature, and the radial stratification of the heavy elements. We also present a model that is consistent with all of the results on the Coma Cluster. In this model the gas is isothermal out to several core radii and is surrounded by a polytropic region.

II. DATA REDUCTION AND ANALYSIS

The instrumentation onboard the X-ray observatory *EXOSAT* (fully described in Taylor *et al.* 1981) consisted of a low-energy telescope (0.1–2 keV) (LE) with a channel multiplier array in the focal plane, and two nonimaging spectrometers (2–10 keV): a gas scintillation proportional counter (GS) and an array of standard proportional counters (referred to as the ME). In this study we have concentrated on the data from the ME (see Turner, Smith, and Zimmermann 1981 for details). Due to higher background and lower sensitivity the GS data for even the bright central pointing are not usable despite the higher energy resolution of this instrument. The signal is weak, statistical errors dominate, and the fractional error on the fitted temperature is about 50%. Although consistent with the ME analysis, the inclusion of these data would not improve our results and will not be discussed further.

The ME array consisted of eight separate proportional counters with two chambers each: one filled with argon and the other xenon. For these observations only the argon detectors showed any significant source signal. The eight detectors were mounted in two halves of four, referred to as H1 and H2. Each half was able to be offset by about 2° from the pointing direction. Background was monitored by alternately offsetting the detectors of each half. This will be discussed in greater detail below. For the Coma observations there was insufficient slew time to use for background estimation.

a) Observations

The data were taken on 1985 Christmas day; a log of observations is in Table 1. Note that each position was observed by both the H1 and H2 halves. The off-center pointings were situated about 45′ from the cluster center in the east, west, and south directions. The northern position was not observed because of two point sources in the *Einstein* image. The eight individual detectors were not precisely coaligned with the satellite pointing direction. The misalignment varied from 4.′4 to as much as 7.′5; the average value was ~5.′7. Observation times have been corrected for dead time using a factor of about 13%. About 2.9×10^5 source counts were collected in the energy range 1–15 keV during the central pointing, while 5.9×10^4, 7.8×10^4, and 8.6×10^4 source counts were collected at the east, west, and south positions. Each individual source and background observation was time series analyzed to search for evidence of flaring. No flares were found. We also tested for a linear variation in rate; all data sets were consistent with slope zero, i.e., constant count rate. Since our main interest in this work was to determine the temperature gradient in the cluster gas, we have taken special care to consider possible sources of systematic error. The most significant sources of systematic error arise from uncertainties in background subtraction and detector gain. We have examined the errors which might arise from variations in both of these quantities and have included these additional errors in our quoted results. Below we discuss each of these.

b) Background Subtraction

During each observation four detectors (that is H1 or H2) observed the source position while the other four detectors monitored the background. After an interval the roles were reversed. Thus each detector had a source pointing and an associated background pointing, which were not contemporaneous. The background observations were carried out in what was known as offset mode. Specifically those detectors monitoring background were offset in pairs 2° away from the given source pointing toward either the NE and NW, or the SE and SW. For this set of observations, all background pointings were carried out to the SE–SW with the single exception of the west pointing using the H2 array, whose background was offset to the NE–NW. Ideally the background positions were source-free regions of the sky. In one case however this was not true, because of the extended nature of the Coma Cluster. The problem occurred for the east pointing for which the background detectors offset in the S–W direction were only about 70′ from the center of the cluster. Significant residual X-ray flux from the cluster was apparent in the background detectors and resulted in much lower count rates and derived fluxes for the (background-subtracted) source pointing. Counters 7 and 8 in H2 were closest to the cluster center and were the most affected. They were not considered in the flux calculation. Quoted fluxes and emission measures for the east pointing are

TABLE 1

EXOSAT OBSERVATIONS OF THE COMA CLUSTER

POINTING	POSITION (1950) α	POSITION (1950) δ	ME SOURCE DETECTORS	OBSERVATION DATE	EXPOSURE TIME (s)
East	$13^h00^m59^s$	28°11′24″	H2	359.60	11510
			H1	359.75	12270
Center	12 57 30	28 11 24	H1	359.90	9260
			H2	360.02	4920
West	12 54 01	28 11 24	H2	360.13	10350
			H1	360.26	10560
South	12 57 30	27 29 24	H1	360.42	9850
			H2	360.55	10200
			H1	360.67	12180

from fits to the data from detectors 1–6 only. None of the other source pointings showed significant indication of a similar problem. Extrapolating the IPC surface brightness profile to the various background fields showed that any flux from the cluster at these radii would be a factor of 15 to 500 less than the corresponding source flux.

An additional complication to the background subtraction procedure was the need to include so-called difference spectra. It has been established that the background spectra of the *EXOSAT* ME detectors changed slightly when counters were placed in offset mode. A large number of observations during the course of the *EXOSAT* mission were used to generate a standard set of difference spectra for each detector and were supplied as part of the analysis software package. To allow for (first order) temporal variations in the difference spectrum over the course of the mission, a correction factor for the overall flux of the difference spectrum was determined by requiring that the net counts above energy channel 60 (approximately 20 keV, where little source contribution is expected) be zero (R. Shafer, private communication). It was found that a factor of 78% of the standard difference spectrum for both halves H1 and H2 was satisfactory for this set of observations of the Coma Cluster. Varying this factor from 68% to 88% did not significantly affect the fitted results. For the offset pointings the ratio of the difference spectrum counting rate to the source counting rate (over the energy band 1–15 keV) was typically 0.04 for the outer counters (1, 4, 5, and 8) and 0.21 for the inner counters (2, 3, 6, and 7). For the central pointing the corresponding ratios were about an order of magnitude smaller than this. Fits to the data from the inner and outer detectors were carried out separately to isolate the effects of the difference spectrum and the derived parameters obtained in each case were in excellent agreement with each other.

The ratios of source count rates to background rates over ~1–15 keV were about 0.90 for the center, while for the east, west, and south the ratios were 0.11, 0.17, and 0.12, respectively. Hence proper background subtraction was a major concern in this project. Variations in the background rate could be the result of a true variation in particle-induced background or could arise from contamination of background pointings by unknown (and unseen) X-ray sources in the field. Note that the LE images were inspected for spurious sources in the four source pointings and nothing significant was found. There were two serendipitous sources in the east pointing, and one each in the center and west pointings, which were detected by the *EXOSAT* standard processing. None was found in the south pointing. For the four detected sources the LE source count rates were all less than 7×10^{-3} counts s^{-1}. Similar images for the 16 background pointings do not exist. However, we are able to estimate the probability that a serendipitous source of nonnegligible intensity would appear in these fields. At the high galactic latitude of Coma such a source is most likely to be an active galactic nucleus with a differential energy spectrum that varies as $E^{-0.6}$ over 2–30 keV (Mushotzky 1984). We consider a source with a flux equal to 0.2 (or more) of the mean of the three off-center fields or about 0.6 counts s^{-1} (2–10 keV). This corresponds to 4.7×10^{-12} ergs cm^{-2} s^{-1} in the 0.3–3.5 keV band where the results of the *Einstein Observatory* medium sensitivity survey (MSS) are expressed (Gioia *et al.* 1984). From the results of the MSS the probability of a source stronger than 0.6 counts s^{-1} appearing in any one field is 0.011. This is small enough to allow us to ignore the source.

In order to estimate the uncertainty in the total background rate we compared the counting rates (1–15 keV) for the several observations available. For H1, the average background counting rate was 30.4 counts s^{-1} and for H2 it was 23.8 counts s^{-1}. The root mean square deviations of the individual rates from these averages were 1.1% and 2.0%. We have taken 1.5% as the uncertainty in the overall background rate. Fits to the data were carried out using the standard value for background and then assuming plus and minus 1.5% of that nominal background. The overall flux of the difference spectrum (see discussion above) was redetermined for these two additional cases and the factors by which the standard difference spectrum were multiplied were 70% (93%) for H1 and 76% (49%) for H2 for the case when the background rate was 101.5% (98.5%) of its standard value.

c) *Gain Variation*

Model fits to proportional counter data are quite sensitive to the intrinsic gain of the detectors and in fact the *EXOSAT* ME detectors did experience some time dependent gain variation over the course of the mission. We were fortunate in that our observations of the Coma Cluster came shortly after a calibration observation of the Crab Nebula on 1985 day 318. In order to test our response function (and gain calibration), we fit an absorbed power law to this calibration data. We derived values of 2.102 ± 0.004 for the power law photon index and $(3.19 \pm 0.12) \times 10^{21}$ atoms cm^{-2} for the column density of absorbing material along the line of sight (90% errors). These parameter values are consistent with published values for the Crab Nebula (Toor and Seward 1974; Koyama *et al.* 1984; Schattenburg and Canizares 1986) and with the values obtained by the *EXOSAT* observatory team (*EXOSAT Express*, **10**, p. 40, 1985 April) for the same data set. Drifts in the gain of the individual ME detectors over the 42 day baseline between the Crab and Coma observations would have resulted in a gain change of from nearly 0 to ~1.6%, with an average change for the eight counters of under 0.3%. However inflight adjustments to the high voltage settings were carried out by the observatory team with the express purpose of keeping the gain of each counter within 0.5% of its nominal value. Based on this, we have used 0.5% as the fractional gain uncertainty associated with the Coma observations. However, this uncertainty really only influences the comparison of the *EXOSAT* results with those of other instruments, i.e., *HEAO 1* A-2 and *Tenma*. Any relative gain difference between the central Coma observation and the off-center ones would be much smaller than this. Thus the ratio of central to off-center temperatures will be considered to be independent of gain uncertainty, but not background uncertainty. On the other hand, the average cluster temperature should include uncertainties arising from both gain and background variations.

d) *Model Fits*

We fitted the data to the optically thin equilibrium ionization X-ray emission models of Raymond and Smith (1977; J. C. Raymond, private communication). The parameters of the fit were temperature, elemental abundance, flux (or normalization), and column density. The column density was fixed at a value of 10^{20} atoms cm^{-2} (Gorenstein *et al.* 1979), although the results are quite insensitive to this quantity. Fits were taken over pulse height channels 4–48 corresponding to the energy range ~0.7–13 keV. The optical redshift of 0.0235 (Sarazin, Rood, and Struble 1982) was included explicitly. For

each PHA bin we added a 1% systematic error in quadrature with the statistical error, a value determined by the *EXOSAT Observatory* team from fits to the Crab Nebula. In addition we varied this error using values of 0%, 1%, and 2%. For the central pointing the best-fit χ^2 values (for 350 degrees of freedom) obtained were 453.6, 411.4, and 328.5, respectively. The total 90% confidence error ranges were 0.51, 0.59, and 0.66 keV for kT and 0.085, 0.093, and 0.101 for fractional cosmic iron abundance (see below). Clearly, increasing the systematic error to as much as 2% would have a negligible effect on our results.

Each observation was fitted by a single temperature, single abundance model. The fitted quantities then represent average cluster values over the *EXOSAT* beam for each direction. Such averages are a simple and straightforward way to approximate multiple spectral components (for *Tenma*, see Hughes *et al.* 1988) and in the case of the *EXOSAT* data analyzed here, yield acceptable χ^2 values. The results can be compared to models by convolving various trial radial distributions for the temperature, iron abundance, and gas density with analytic forms for the *EXOSAT* collimator response. This is discussed in § III below.

We fitted each detector separately with the same temperature and abundance, letting each normalization vary freely. The variation in flux from detector to detector for the same pointing was about 5 times larger than the statistical errors would predict. This is a result of slight differences in the collimators and pointing directions for the several detectors. In addition (as discussed above) background subtraction may vary somewhat from detector to detector. The errors we associate with flux (and emission measure) include these additional sources of error.

Since the detectors are independent, we have added the χ^2 values for corresponding values of temperature and abundance for the eight detectors in each pointing. Our results are in Table 2. The errors shown are 90% confidence for a single parameter. In deriving emission measures we have used a value of 50 km s^{-1} Mpc^{-1} for the Hubble constant, implying a distance of 140 Mpc to the Coma Cluster. The quoted iron abundances are relative to the cosmic value of 4.0×10^{-5} iron atoms per hydrogen (Allen 1973). Note that the abundances of elements with $Z > 2$ (specifically C, N, O, Ne, Mg, Si, S, Ar, Ca, Fe, and Ni) were varied from their cosmic values by this same factor. The He/H ratio was kept fixed. Figures 1–4 show plots of the data and best-fit models for the four pointings. For just

TABLE 2

RESULTS OF FITS TO *EXOSAT* ME DATA FOR THE COMA CLUSTER

Pointing	kT (keV)	Abundance[a]	n^2V[b] (10^{67} cm^{-3})	χ^2/ν
Center[c]	$8.50^{+0.31}_{-0.37}$	0.20 ± 0.04	6.23 ± 0.37	411.4/350
East[d]	$7.78^{+1.27}_{-0.98}$	$0.27^{+0.24}_{-0.19}$	0.87 ± 0.33[e]	346.7/350
West[d]	$7.65^{+0.81}_{-0.71}$	$0.09^{+0.11}_{-0.09}$	1.25 ± 0.18	345.9/350
South[d]	$6.82^{+0.79}_{-0.66}$	$0.23^{+0.20}_{-0.12}$	0.71 ± 0.09	339.9/350
Average Off-Center[c]	$7.39^{+0.68}_{-0.76}$	$0.17^{+0.09}_{-0.10}$	...	1037.8/1054

[a] Fraction of cosmic value (4.0×10^{-5} iron atoms per hydrogen).
[b] $H = 50$ km s^{-1} Mpc^{-1}.
[c] Error from 1.5% background variation added in quadrature to statistical error.
[d] Statistical errors only.
[e] Detectors 1–6 only.

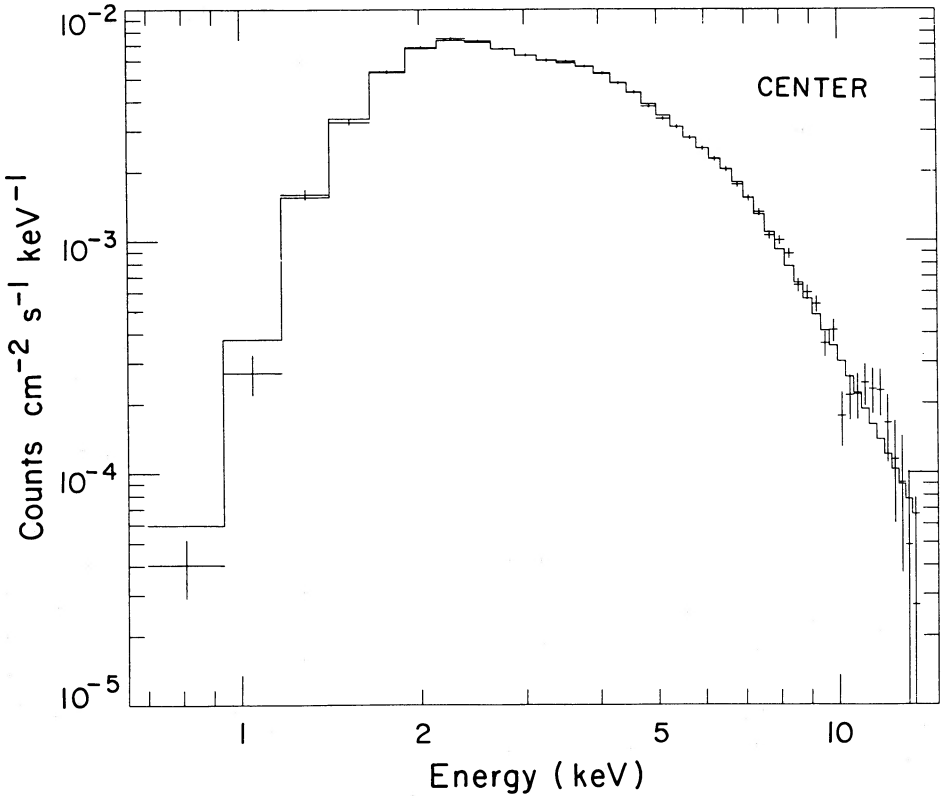

FIG. 1.—*EXOSAT* ME X-ray spectrum for the center pointing of the Coma Cluster with best-fit single-temperature, single-abundance thermal model

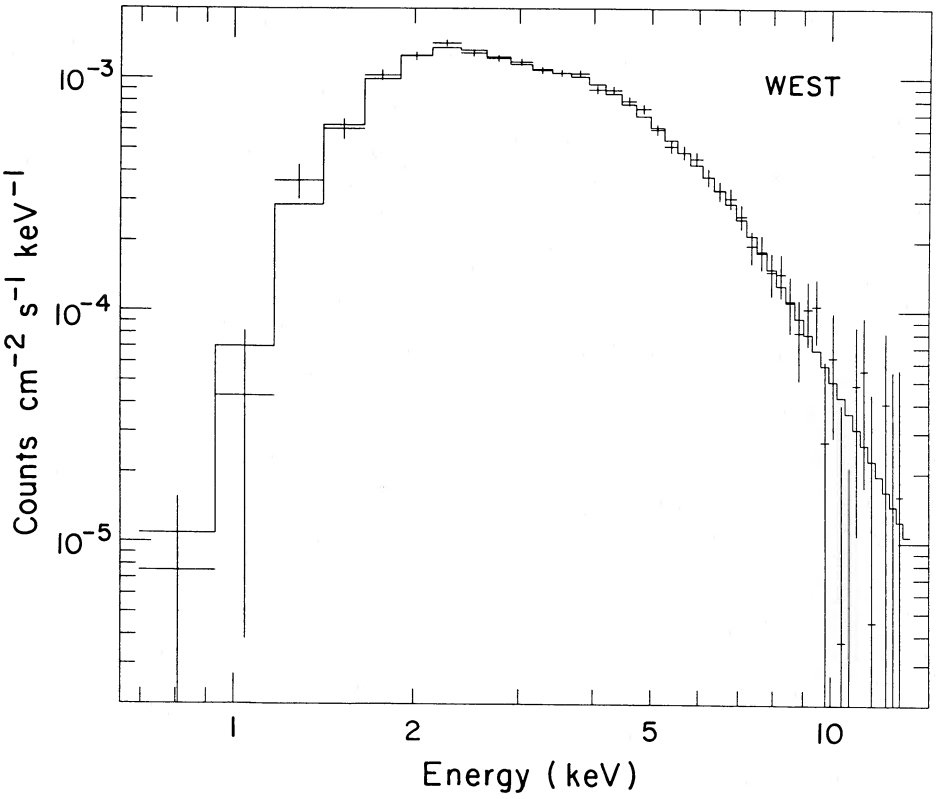

FIG. 2.—Same as Fig. 1 but for the west pointing of Coma

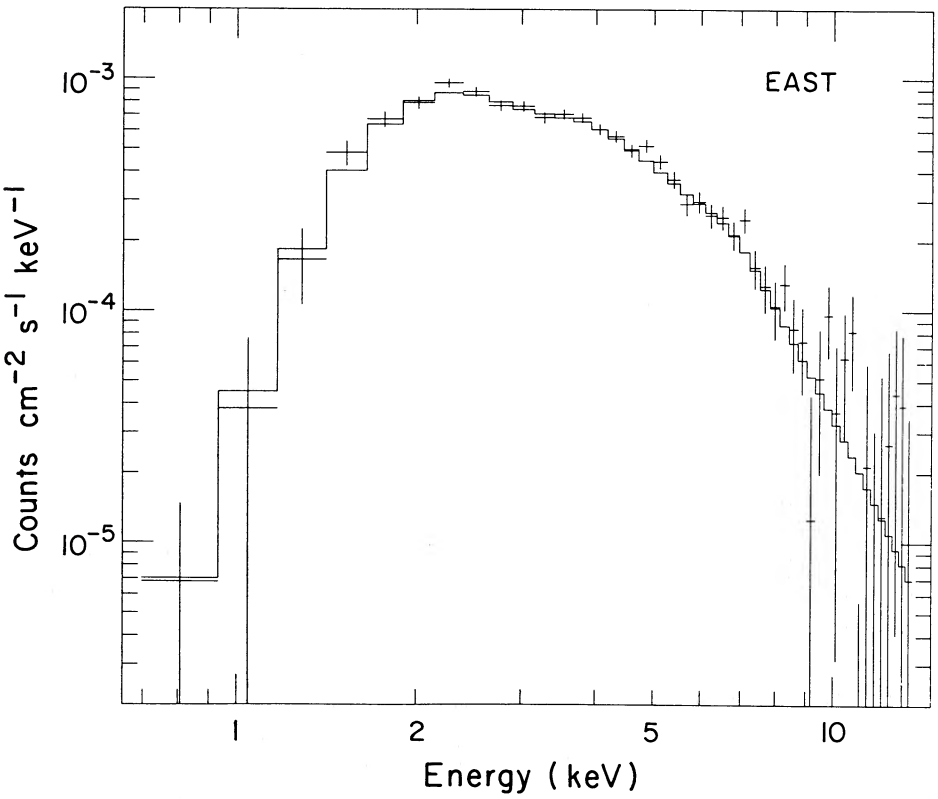

FIG. 3.—Same as Fig. 1 but for the east pointing of Coma

this graphical presentation, the data and model from the eight individual detectors were summed for each pointing to produce the displayed composite spectra.

The center pointing yielded a χ^2 value which was somewhat high, 411.4 for 350 degrees of freedom, which can be rejected at a confidence level of about 99%. However this arose primarily from a poor fit for detector 5. Both the background subtraction and detector gain were varied separately for this individual data set but there was no improvement in the fit. Excluding this detector from the ensemble for the center pointing gave a total χ^2 of 329.3 for 306 degrees of freedom, which can be rejected at only less than 83%. Meanwhile the fitted values of temperature and abundance were not changed significantly, except for a proportional increase in statistical error. Rather than exclude detector 5 from all the pointings, we have chosen to accept this larger value of χ^2 for the central pointing. We stress that this does not arise from our approximation of a single temperature, single abundance model for fits to the data.

The three off-center pointings gave acceptable χ^2 values and the derived parameters are in agreement with each other. There was no noticeable problem with detector 5 here. To improve our sensitivity to radial variations in temperature and abundance, we added the χ^2 maps for the east, west, and south pointings to determine an off-center average. Parameter values are shown in the final line of Table 2.

In order to investigate the significance of the iron line detections we fitted the data using a value of zero for the heavy element abundance. In this case the best-fit kT values were 9.3 keV for the center and 7.9 keV for the off-center average and the corresponding χ^2 values were 471.8 (351 degrees of freedom) and 1049.3 (1053 degrees of freedom). The ratio of the difference in χ^2 to the best-fit reduced χ^2, $F_\chi = \Delta\chi^2/\chi_\nu^2$, which follows the F distribution (Bevington 1969), gives us a measure of the confidence we have in introducing an additional parameter, here the iron abundance. For the center observation, $F_\chi = 51.4$ implying a confidence level well in excess of 99.95% for the introduction of the iron abundance parameter. The off-center observation yields $F_\chi = 11.7$, which is somewhat less significant (confidence level of $\sim$99.9%). It is clear that iron emission lines are present in both spectra. We show this graphically in the residuals spectra (Figs. 5 and 6), where the best-fit continuum has been subtracted. For the center observation the iron emission lines show up as a large excess between 6 and 7.5 keV. This peak is more than 8 standard deviations from zero. For the off-center observation, the flux in this energy range is greater than zero by about 4 standard deviations. No other feature of comparable width appears in this spectrum at a significance greater than 2 σ.

Two-dimensional χ^2 maps of temperature versus abundance for the off-center average, as well as the center pointing are shown in Figure 7. The 68%, 90%, and 99% confidence contours for two interesting parameters ($\chi_{min}^2 + 2.30$, $\chi_{min}^2 + 4.61$, $\chi_{min}^2 + 9.21$; Avni 1976; Lampton, Margon, and Bowyer 1976) are displayed. Clearly the off-center average has a lower temperature than does the central region, while the iron abundance is consistent with being the same. However this figure includes only statistical errors; to make quantitative statements about the significance of any temperature or abundance variation requires the inclusion of additional error terms.

We carried out fits to the data in exactly the same manner as above, but with the total amount of background increased and decreased by 1.5% as previously discussed. The best-fit kT

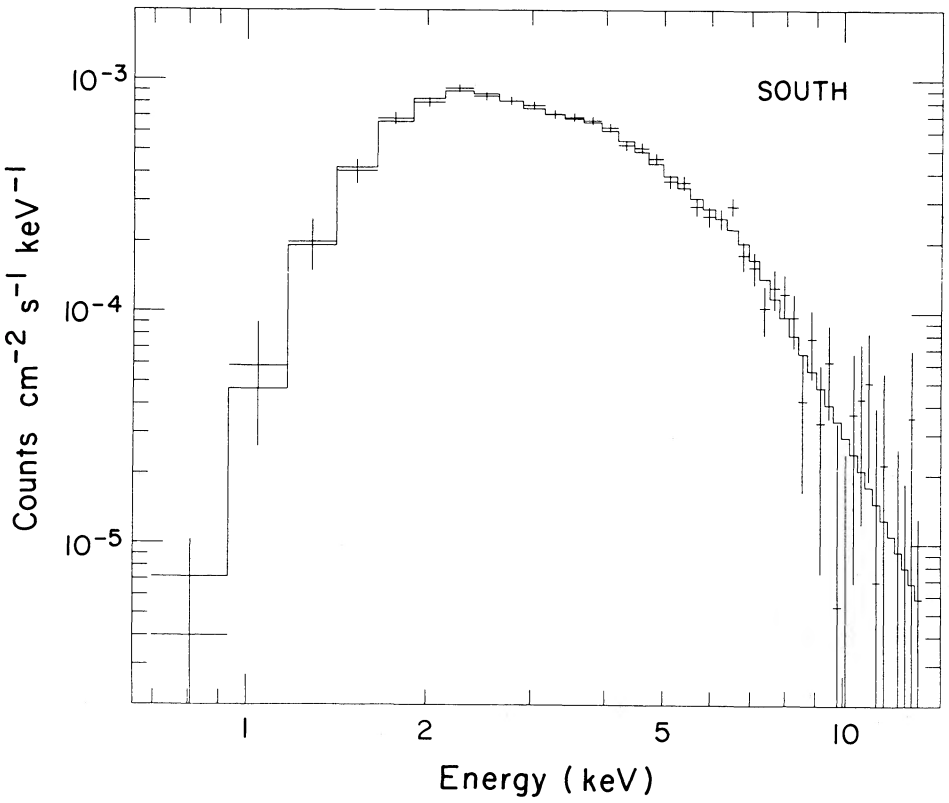

FIG. 4.—Same as Fig. 1 but for the south pointing of Coma

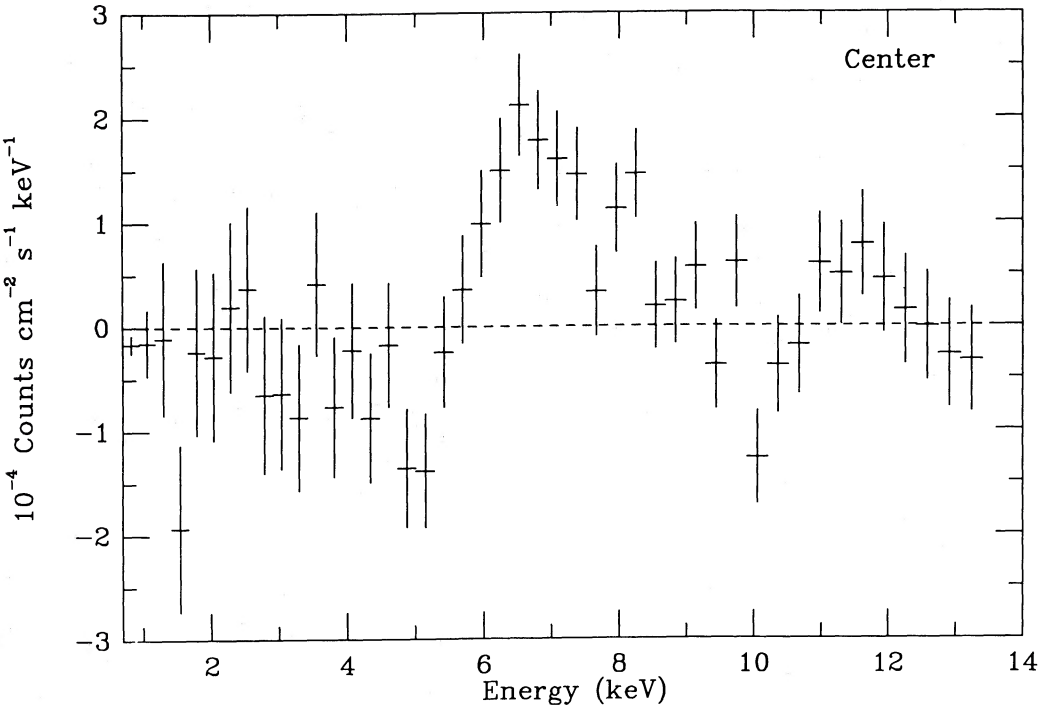

FIG. 5.—Residual spectrum for the center observation of Coma after the best-fit continuum model was subtracted. K-shell iron emission lines are prominent between 6 and 7.5 keV.

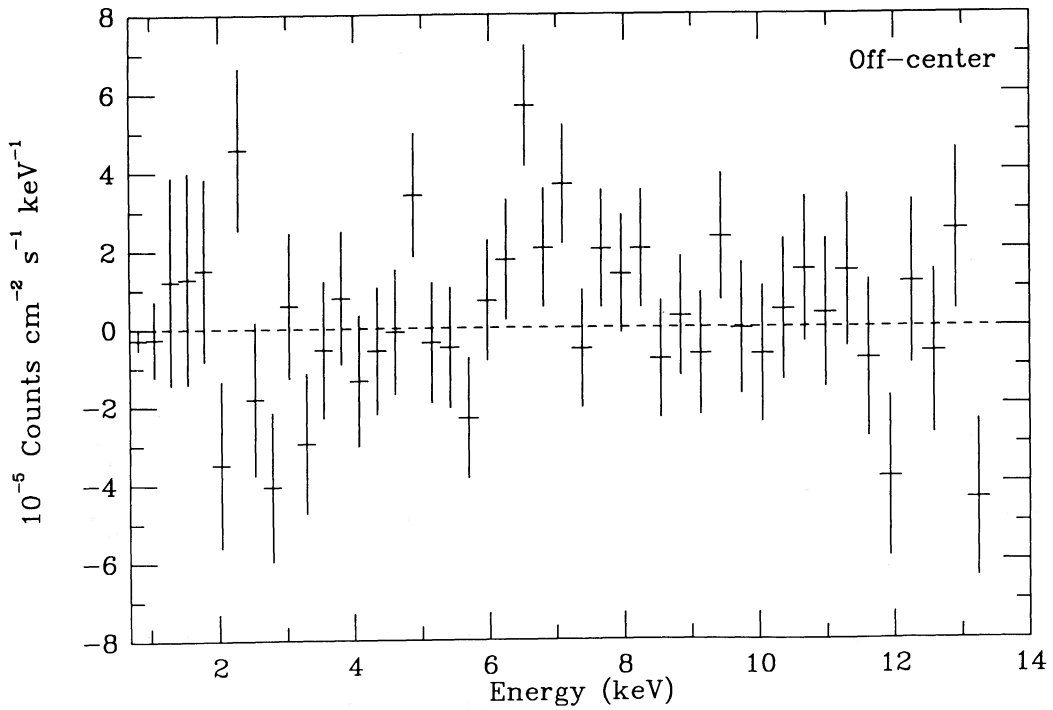

FIG. 6.—Same as Fig. 5 but for the off-center average

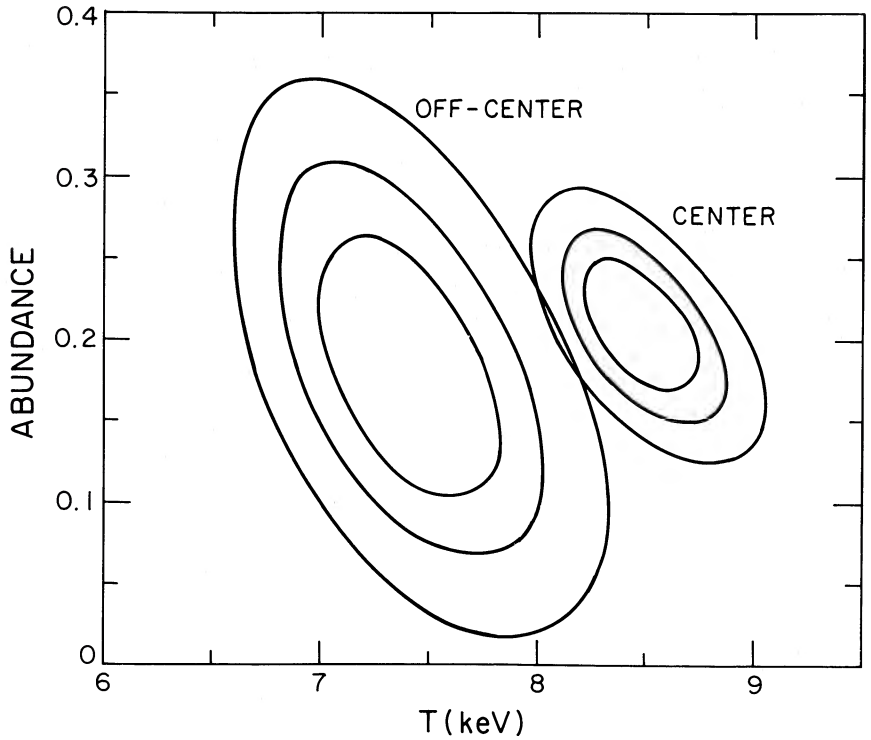

FIG. 7.—Results of fits to the *EXOSAT* X-ray spectra of Coma. Two-dimensional χ^2 contours (68%, 90%, and 99% confidence levels) for fractional iron abundance vs. temperature. The cosmic iron abundance is assumed to be 4.0×10^{-5} relative to hydrogen. The contours at the right are from the center pointing, while the contours on the left are the off-center average.

changed by +0.09 keV (for 0.985 background subtraction) and −0.22 keV (for 1.015 background subtraction) for the central pointing and +0.46 keV and −0.57 keV for the average of the off-center pointings. At the same time the iron abundance changed by +0.004 and −0.017 (center) and +0.026 and −0.066 (off-center average). These additional quantities were added in quadrature with the statistical errors to produce the final errors shown in Table 2. These parameter values and errors can be used to define ratios (with errors) of temperature, abundance, and emission measure between the center and off-center regions. We do this below. Such ratios should be independent of small changes in the detector gain calibration. However possible gain variations do apply to the absolute temperature or abundance determination. When the gain of the detectors was varied by −0.5% to +0.5%, we found the best-fit kT for the central pointing changed by +0.34 keV and −0.37 keV, and the iron abundance changed by −0.010 and +0.016. These values are to be added in quadrature with the errors on the parameters for the central pointing alone in order to compare to previous results.

In Figures 8 and 9, we compare the center and off-center fitted values of temperature and abundance. These figures were constructed by computing a χ^2 statistic in the following manner. For a given value of temperature or abundance along either the center or off-center directions in the figures, we calculated a quantity which was the difference between that trial value and the measured value from Table 2, divided by the corresponding (1 σ) error. Then at each point in the parameter space, our χ^2 statistic was just the sum of the squares of this quantity in the two directions. The displayed contours are at the 68%, 90%, and 99% confidence levels ($\chi_{\min}^2 + 1.00$, $\chi_{\min}^2 + 2.71$, $\chi_{\min}^2 + 6.63$; Avni 1976; Lampton, Margon, and Bowyer 1976) for a single interesting parameter (since we wish to determine limits on the parameter ratios alone). In each figure the dashed line represents the case when the center and off-center values are equal, i.e., when the ratio equals 1. Figure 8 shows that the temperatures are different at a confidence level somewhere between 90% and 99%. In contrast, the iron abundance (Fig. 9) is entirely consistent with a uniform value. Table 3 presents our final results for the center temperature and the ratio of center to off-center temperatures and the corresponding quantities for the iron abundance. The errors quoted here are 68% ($\sim 1\ \sigma$) and for the center values include the effects of detector gain variation added in quadrature. The errors on the ratios come from the 68% confidence level contours of Figures 8 and 9. It is now possible to use these derived values in conjunction with those obtained by other instruments. We do such comparisons in § III below.

We have used the same technique to determine the ratio of emissivity from the center to the various off-center pointings. Table 4 contains these ratios, as well as the pointing distance from the cluster center. The effective radius sampled by each pointing is also shown. The measured 2–10 keV X-ray fluxes in each of the pointings are given too.

TABLE 3

FINAL RESULTS FOR X-RAY TEMPERATURE AND FRACTIONAL IRON ABUNDANCE

Parameter	Center Value	Ratio: Center to Off-center
kT (keV)	$8.50^{+0.28}_{-0.32}$	$1.150^{+0.083}_{-0.069}$
Iron abundance	$0.20^{+0.025}_{-0.025}$	$1.18^{+0.72}_{-0.31}$

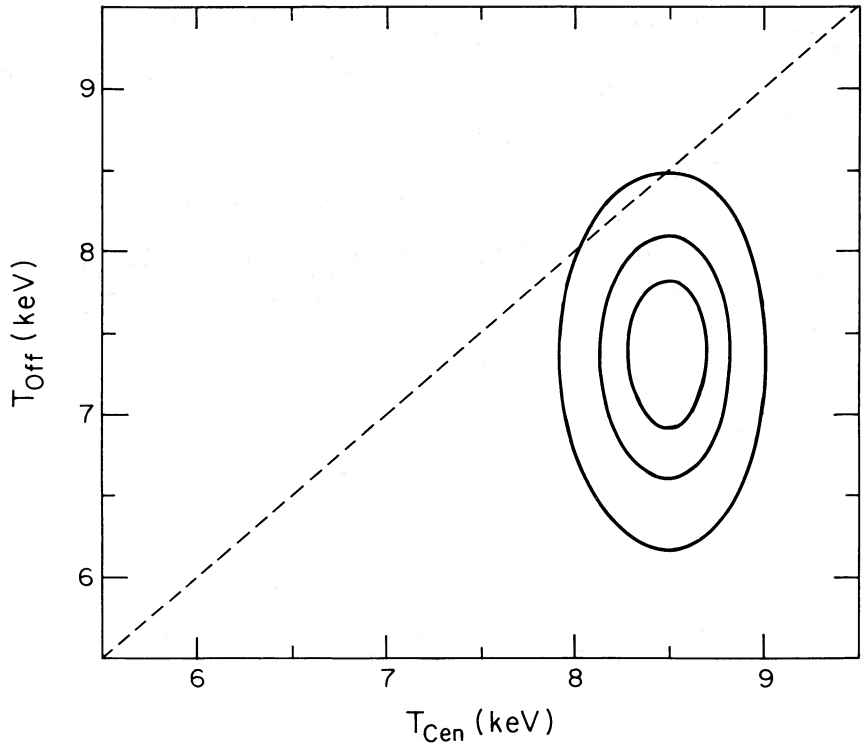

FIG. 8.—Two-dimensional χ^2 contours of center temperature vs. off-center temperature at 68%, 90%, and 99% confidence. The dashed line corresponds to equal center and off-center temperatures.

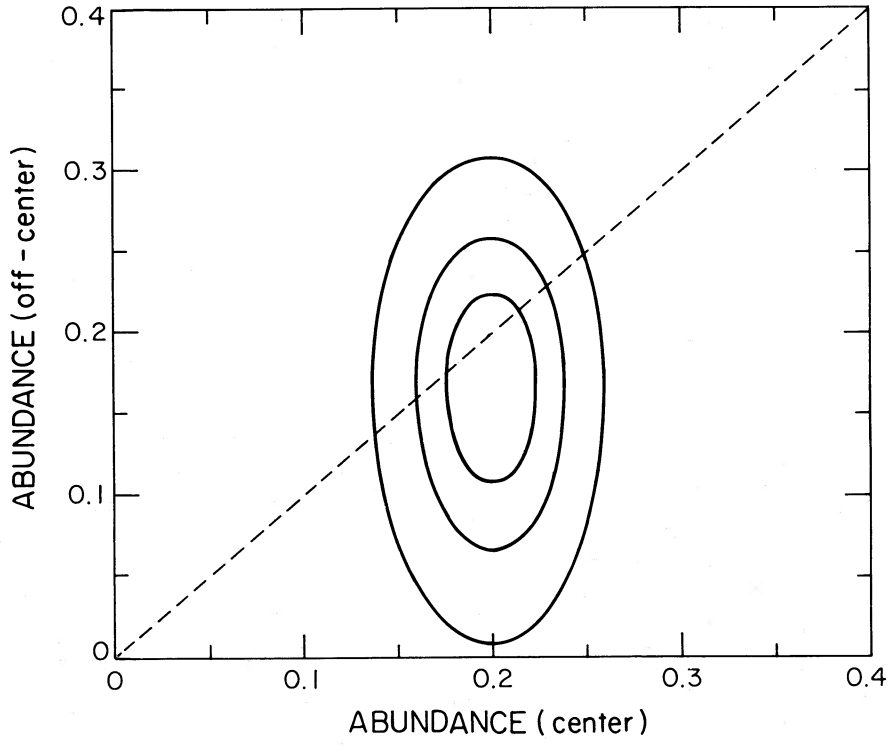

FIG. 9.—Same as Fig. 8, but for the iron abundance

TABLE 4

COMA CLUSTER X-RAY FLUXES

Pointing	Distance from Center[a]	Effective Radius	Flux (2–10 keV) (10^{-10} ergs cm^{-2} s^{-1})	Ratio to Center
Center	6.8	11′	2.72 ± 0.15	...
East	44.3	19	0.378 ± 0.135[b]	0.147 ± 0.033
West	48.5	25	0.494 ± 0.071	0.196 ± 0.019
South	48.5	23	0.285 ± 0.034	0.114 ± 0.010

[a] Cluster center at $12^h57^m19^s$, 28°13′7″.
[b] Detectors 1–6 only.

Finally we wish to discuss the significance of our temperature determination. First we assume that the cluster temperature is uniform throughout. In this case using the center and off-center temperatures in Table 2 we determine a χ^2 of 5.3 for 1 degree of freedom with a best-fit isothermal kT of 8.25 keV. This can be rejected with greater than 97.5% confidence. However, if the observed cluster kT from the *Tenma* satellite, 7.5 ± 0.2 keV, is included as well, we obtain a χ^2 of 11.7 for 2 degrees of freedom and an average isothermal kT of 7.78 keV. This can be rejected at greater than 99.5% confidence. These combined data sets present strong evidence for nonisothermality of the gas in the Coma Cluster. Below we show that the *Tenma* and *EXOSAT* data are entirely consistent with a large class of nonisothermal models.

III. A POTPOURRI OF MODELS

In this section, we carry out a detailed comparison between the results obtained above and models for the spatial variation of temperature, iron abundance, and surface brightness in the cluster. For this purpose, we generated a model transmission function (beam pattern) for each of the four pointings. The basic function consisted of a pyramidal model for the rectangular collimator with a flat top response 6.9 in width and a linear falloff of 49.7 (FWHM). Beyond ~46.3 the response is zero. This calibration function was determined before launch and was found to be consistent with inflight calibration observations (*EXOSAT* Observers Guide, Part III, Rev 2, Sect 8.2). In particular there is no evidence for a reflection effect leading to a broader response. We have included the satellite roll angle and the average detector misalignments from the targeted direction in our calculation as well. The cluster center is taken to be that given in Abramopoulos, Chanan, and Ku (1981), $\alpha_{1950} = 12^h57^m19^s$, $\delta_{1950} = 28°13'07''$.

a) *Surface Brightness Models*

Ratios of center and off-center emissivities were used to set limits on the radial surface brightness variation. The Coma Cluster is clearly elliptical, with the major axis aligned approximately in the east-west direction (Chanan and Abramopoulos 1984). We averaged over this ellipticity by taking the average of the east and west flux ratios, then averaging that with the south to get a value of 0.149 ± 0.013. The model is based on a radial gas density variation given by

$$n(R) = n_0[1 + (R/R_{\rm core})^2]^{-3\beta/2}, \quad (1)$$

the so-called isothermal beta model (Cavaliere and Fusco-Femiano 1976; Sarazin and Bahcall 1977; Gorenstein *et al.* 1978). The scale length is $R_{\rm core}$ and β is the dimensionless temperature, $\beta = \mu m_p \sigma^2/kT$, where σ is the galaxy line-of-sight velocity dispersion. Optical data for the Coma Cluster (Kent and Gunn 1982) yield $\sigma \approx 1000$ km s^{-1}. Combined with our average isothermal kT of ~7.8 keV, we expect $\beta \approx 0.8$.

Surface brightness profiles were generated using the given density profile and an isothermal temperature distribution over the parameter plane of $R_{\rm core}$ versus β. The profiles were then convolved through the *EXOSAT* beam pattern for the four pointings and the off-center values were averaged using the same procedure as for the data. A χ^2 value was assigned to each model using the average derived ratio of 0.149 ± 0.013 as a single data point. Our results are in Figure 10, which shows the 68%, 90%, and 99% confidence contours as bands extending across the $R_{\rm core}$ direction.

Also shown in Figure 10 are the results of fits to the X-ray surface brightness data from the imaging proportional counter (IPC) on the *Einstein Observatory* (Giacconi *et al.* 1979). Two sets of data corresponding to two different regions were used. See Hughes *et al.* (1988) for details of these data. The larger closed contours on the right side of the figure correspond to the data from an azimuthal average over radii from 0′ to 20′. The smaller closed contours on the left come from a larger radial region (0′–40′) extending toward the northern quadrant, where there was an additional observation by the IPC. The *EXOSAT* results are in excellent agreement with both IPC data sets, but it is clear that the most stringent constraints still arise from the *Einstein* imaging data.

The overall normalization to the *EXOSAT* data from the center pointing can be used to determine the central density in equation (1). This calculation depends on the assumed value of $R_{\rm core}$ and β. In Figure 11 we plot the model central density n_0 (number density of hydrogen atoms) versus $R_{\rm core}$. The upper (lower) curve here corresponds to values of β taken from the 68% upper (lower) limit in Figure 10. The best-fit value from the *Einstein* IPC data is shown as the cross. Considering the uncertainties in the absolute efficiency of X-ray detectors, the agreement is certainly adequate.

b) *Temperature Models*

In a previous paper in which the *Einstein* IPC data and *Tenma* spectral data for Coma were analyzed jointly (Hughes *et al.* 1988), conventional polytropic models for the temperature distribution (Cavaliere and Fusco-Femiano 1976, 1978; Bahcall and Sarazin 1978) were found to be unsatisfactory. Such models assume that the radial temperature distribution follows the gas density distribution as a power law, $T(r)/T_0 = [n(r)/n_0]^{\gamma-1}$, where γ is the polytropic index. The most consistent model for the X-ray emission was one with an isothermal central region surrounded by a decreasing polytropic temperature distribution, which was designated the hybrid model. An isothermal region of kT ~8–12 keV extending out 1 to 6 core radii yielded the best solution. However, this result relied largely on fits of a specific model to the *Tenma*

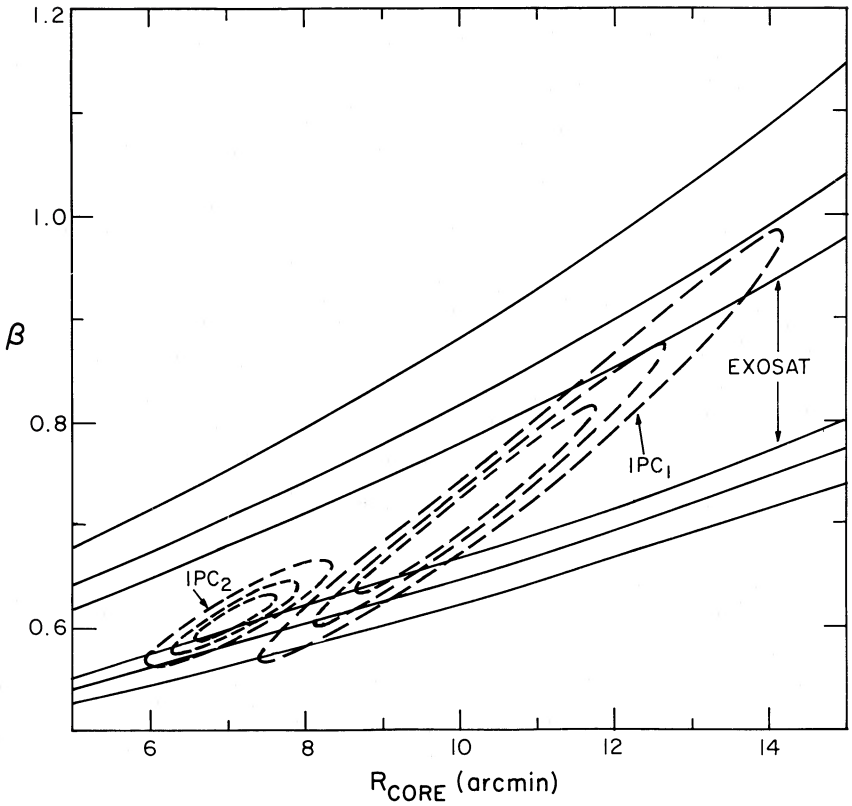

FIG. 10.—Two-dimensional χ^2 contours of core radius vs. β at 68%, 90%, and 99% confidence. The limits from the *EXOSAT* data are the bands running across the figure. The limits from the IPC data are the closed dashed contours and correspond to two different regions in the cluster.

spectral data and could not be considered definitive. Models with a positive temperature gradient (i.e., a lower temperature in the center relative to the edge) and ones where the temperature variation was not a global effect (e.g., a model with cooler regions embedded in a hotter matrix) really could not be eliminated. Now, however, such models can be eliminated with some confidence using the *EXOSAT* results. The temperature variation in the Coma Cluster has a definite radial variation with a negative gradient.

We have also compared the temperature results directly to the hybrid model discussed above. An average temperature, weighted by surface brightness and the appropriate collimator response, was determined for each of the *EXOSAT* pointings for a large number of values of the parameters R_{iso} and T_{iso} (the radius and temperature of the isothermal central region of the hybrid model). The model surface brightness parameters were fixed at $R_{core} = 6'.9$ and $\beta = 0.60$, and the polytropic index in the region beyond R_{iso} was set to 1.555. These were the same values as used in Hughes *et al.* (1988). Contours of constant χ^2 in the R_{iso}-T_{iso} parameter plane were generated by comparing the model values for center temperature and temperature ratio with the fitted values from Table 3. A contribution to the χ^2 value from the ratio of center to off-center fluxes was also included. The results are displayed in Figure 12, where the 68%, 90%, and 99% confidence contours are shown as solid curves. The results of fits to the *Tenma* data using the identical model are shown as the dashed contours (68% and 90%). These are in excellent agreement and imply that the isothermal region of Coma extends out to ~2–6 core radii with a kT of 8–10 keV. This corresponds to a linear radius of from 0.6 Mpc to 1.7 Mpc, within which about 40% to 75% of the total emission measure from the Coma Cluster arises.

c) *Iron Abundance Models*

Our measured values of iron abundance allow us to test the model of Abramopoulos, Chanan, and Ku (1981) (hereafter ACK) for the distribution of the elements in the Coma Cluster. Briefly, these authors calculate the spatial distribution of all the different chemical elements in the gravitational potential well of the cluster under the assumption that there has been sufficient time to reach the equilibrium distribution. They determine that the heavier elements are distributed preferentially toward the center of the cluster, and that virtually all of the iron is contained within less than one core radius. Their equilibrium model was found to be consistent with the imaging data from the IPC and yielded an average apparent iron abundance of 0.35, which was the current value at the time (Mushotzky *et al.* 1978). The actual abundance of iron within the cluster, however, was some 20 times less than this. On the other hand, Rephaeli (1978) calculated the rate at which heavy ions settle in the cluster potential and found that the ion drift time was quite large, $\sim 10^{11}$ yr from distances of about four core radii to within one core radius for parameters appropriate to the Coma Cluster. Thus it is unlikely that the equilibrium distribution of elements has been established within the cluster. Yet an abundance gradient in the intracluster medium could be the result of other processes. For example, the mass lost from stars within galaxies would be enriched in heavy elements and might be preferentially deposited in the cluster core through the action of ram pressure or collisional stripping.

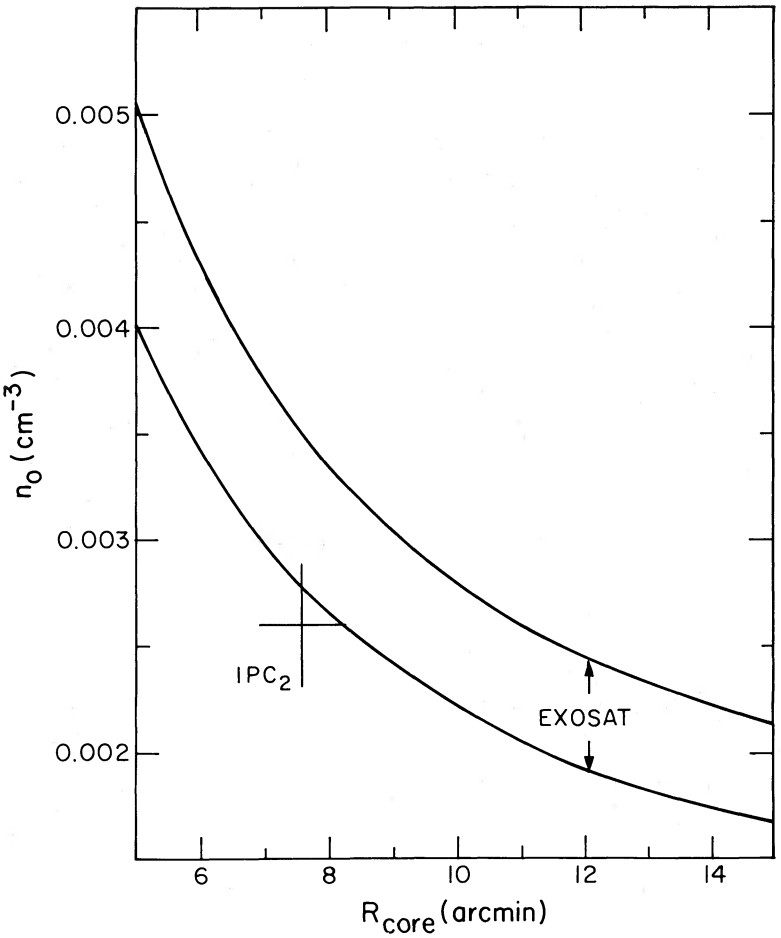

FIG. 11.—Central density (number of hydrogen atoms) vs. core radius from the normalization to the *EXOSAT* center pointing. The cross is the IPC value.

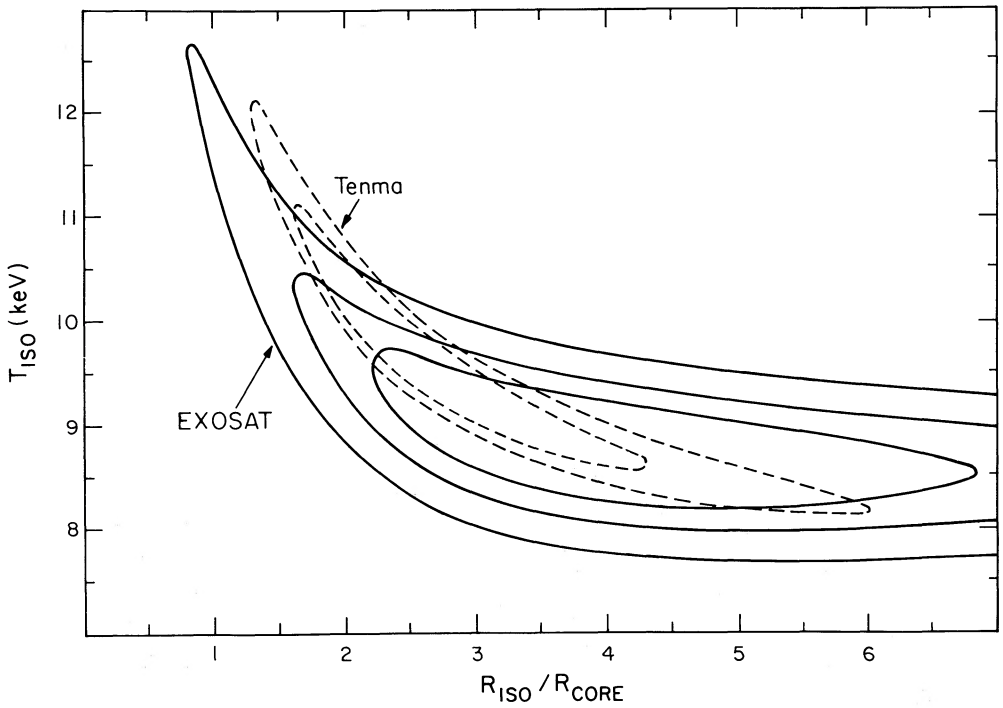

FIG. 12.—Results of fits to the hybrid model, consisting of an isothermal core surrounded by a polytropic distribution. We display two-dimensional χ^2 contours for the temperature of the isothermal region (T_{iso}) vs. its radius (R_{iso}) in units of the core radius. The *EXOSAT* temperature results are shown as the solid curves (at the 68%, 90%, and 99% confidence levels), while the dashed curves are from fits of the identical model to the *Tenma* spectral data (only the 68% and 90% contours are drawn).

However, in the absence of any specific model predictions for such an abundance gradient, we will be content with a comparison to the ACK model.

We have three measurements of the iron abundance: the *Tenma* value, and the *EXOSAT* center and off-center values. The *Tenma* value, 0.21 ± 0.018, represents the global average from the cluster, since it was obtained from a large field of view (3°). This value is consistent with those obtained by *OSO 8* and *HEAO 1* A2, 0.25 ± 0.07 and 0.21 ± 0.04 (Henriksen and Mushotzky 1986), although the *Tenma* value is considerably more precise. We convolved the ACK partially processed equilibrium model ($\epsilon = 0.047$) through the *EXOSAT* collimator response and obtained an abundance of 0.25 for the center and 0.09 for the off-center regions, while the global average was 0.17. These values have been scaled to allow for a different apparent abundance than ACK used. If we just consider the *EXOSAT* measurements in Table 3, we can reject the ACK model at about 95% confidence. However, when the *Tenma* value is included to represent the global average of the iron abundance, we obtain a χ^2 of 13.5 for 2 degrees of freedom, which requires us to reject the model with greater than 99.5% confidence. Alternatively, a uniform abundance of 0.20 yields a χ^2 of only 0.4 for the same number of degrees of freedom.

We have introduced a simple model for the iron distribution in order to quantify just how spatially uniform the abundance must be. The model assumes that the iron is distributed uniformly within a given radius $R_{\rm Fe}$ and is entirely absent beyond. A plot of the χ^2 values versus $R_{\rm Fe}$ is shown in Figure 13 for this model and the combined *EXOSAT* and *Tenma* abundance measurements. The confidence levels shown are for a single interesting parameter. The best fit occurs when the heavy elements are distributed uniformly throughout the whole cluster. However, at 90% confidence our data allow a model in which the iron is confined to a region within about 3.6 core radii ($\sim 28'$) of the cluster center. It is clear that the distribution of heavy elements in the Coma Cluster is approximately uniform within at least four core radii of the center.

IV. PHENOMENOLOGICAL MODEL OF THE COMA CLUSTER

In this section we present a simple phenomenological model for the hot plasma in the Coma Cluster. The gas density distribution is well expressed by equation (1) with $\beta = 0.63 \pm 0.03$, $R_{\rm core} = 7'.6 \pm 0'.7$, and $n_0 \sim 3 \times 10^{-3}$ cm^{-3} (Hughes *et al.* 1988). The gas temperature distribution is poorly represented by a purely polytropic model (Cavaliere and Fusco-Femiano 1976, 1978; Hughes *et al.* 1988); the best-fit *Tenma* and *EXOSAT* combined χ^2 for this polytropic model was 81.4 for 52 degrees of freedom. Instead a hybrid model, which is isothermal within a certain radius and then polytropic beyond, gave a greatly improved fit: χ^2 of 66.0 for the same number of degrees of freedom. The temperature distribution used was

$$T(R) = \begin{cases} T_{\rm iso} & R \le R_{\rm iso} \\ T_{\rm iso}\left[\dfrac{1 + (R/R_{\rm core})^2}{1 + (R_{\rm iso}/R_{\rm core})^2}\right]^{-3\beta(\gamma-1)/2} & R > R_{\rm iso} \end{cases} . \quad (2)$$

The best-fit values and 90% errors for the combined *Tenma* and *EXOSAT* data sets are $R_{\rm iso} = 23^{+12}_{-8}$ arcmin and $T_{\rm iso} = 9.1 \pm 0.7$ keV. In Figure 14 a plot of the best-fit gas density and temperature distributions are shown as a function of radius. In addition the 99% confidence contours exclude both a pure polytropic model (with $\gamma = 1.555$) as well as a pure isothermal

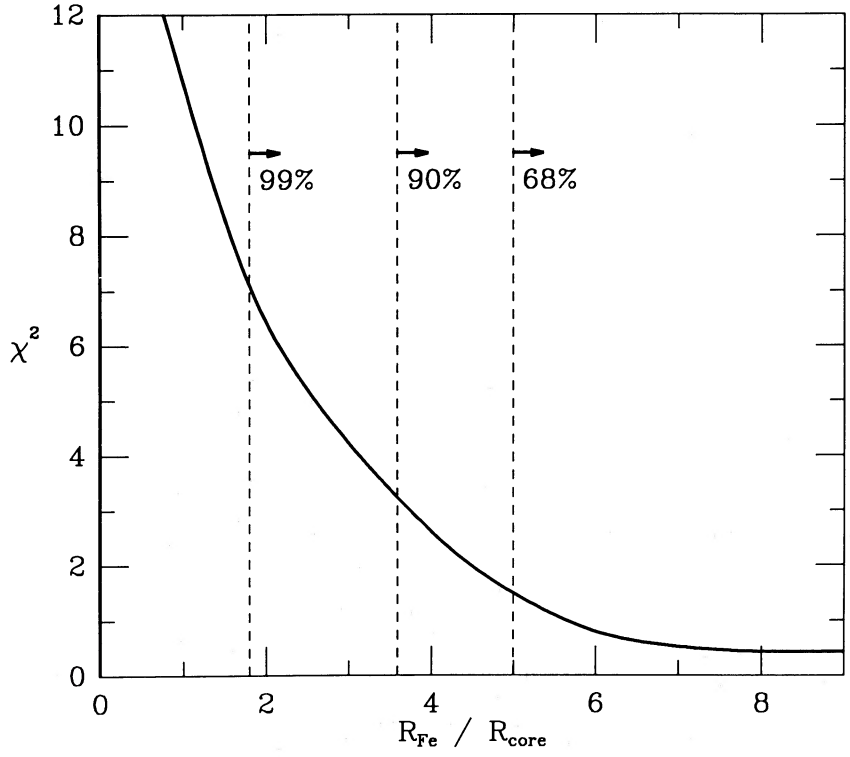

FIG. 13.—Results of fits to a model with uniform iron abundance within radius $R_{\rm Fe}$. The 68%, 90%, and 99% confidence levels for a single interesting parameter are shown. Clearly most of the cluster is required to have a uniform iron abundance.

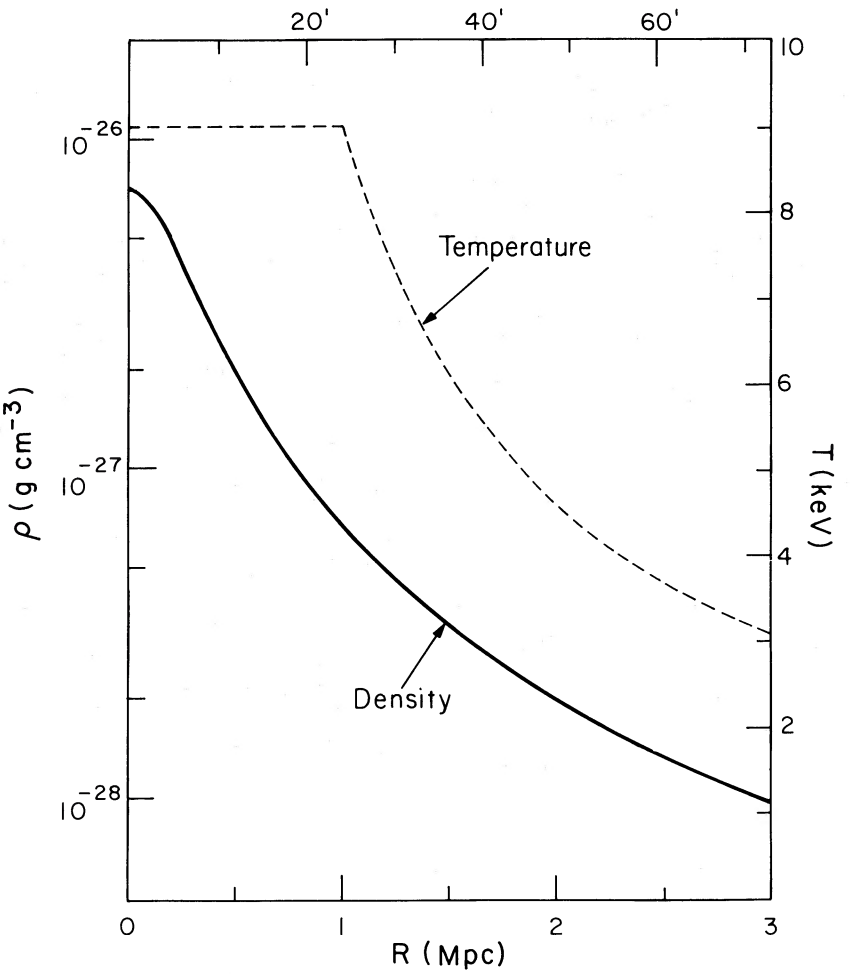

FIG. 14.—Phenomenological model of the gas in the Coma Cluster. Gas temperature (*dashed*) and mass density (*solid*) are plotted vs. radius. The temperature scale is on the right and the density scale is on the left. Both angular (*top*) and linear (*bottom*) radial scales are shown, corresponding to a distance of 140 Mpc.

model. Finally the distribution of iron in the cluster is nearly uniform within a radius of at least 28′ of the center.

V. CONCLUSIONS

We have explored the radial variation of temperature and iron abundance for the plasma in the Coma Cluster of galaxies. Our principal results are summarized below.

1. Comparison of the *EXOSAT* and *Tenma* results leads us to conclude that the Coma Cluster almost certainly deviates from isothermality. In addition, since the *EXOSAT* data come from different positions in the cluster, the observed temperature variation truly must be a global phenomenon. Nevertheless the temperature variation is quite modest and a model with an isothermal core surrounded by a decreasing temperature distribution can describe adequately all of the Coma data, both spectral and imaging.

2. The spatial distribution of the heavy elements in Coma is approximately uniform and the equilibrium distribution of Abramopoulos, Chanan, and Ku (1981) can be rejected with high confidence. There seems to be no compelling reason now to doubt the existence of large amounts of highly processed gas within the intracluster medium of the Coma Cluster and indeed other clusters of galaxies.

In a forthcoming paper (Hughes 1988), we employ all the available X-ray data, in particular the results on temperature presented here, to set limits on the mass distribution of the cluster. Comparison with the results of such studies for the optical data (The and White 1986; Merritt 1987), will be presented as well.

The total mass of X-ray emitting gas in the Coma Cluster is $\sim 2.0 \times 10^{14}\ M_\odot$ within 2 Mpc ($\sim 50'$) and $\sim 5.6 \times 10^{14}\ M_\odot$ within 5 Mpc ($\sim 120'$), with a fractional uncertainty on these measurements of about 10%. We have shown above that the iron abundance is uniform at a value of 8×10^{-6} per hydrogen atom. Thus the mass of iron is $\sim 0.6 \times 10^{11}\ M_\odot$ (2 Mpc) and $\sim 1.8 \times 10^{11}\ M_\odot$ (5 Mpc). De Young (1978) studied the production of iron-enriched gas in clusters of galaxies and found that $\sim 1.5 \times 10^{11}\ M_\odot$ of iron would be lost from the stars in the cluster galaxies over the last 10^{10} yr. However, not enough total mass is ejected from the galaxies in this model to account for the observed continuum X-ray emission. In fact, since most of the processed matter from stars comes off with greater than solar abundances, it is not surprising that the total gas mass is too low. Clearly some dilution with primordial matter is necessary in order to produce the observed heavy element abundance of $\sim 20\%$. We find that within about 5 Mpc, De Young's model (and indeed virtually any model in which the gas is injected with enhanced abundances) requires that 85% to 95% of the intracluster gas be primordial. Perhaps the polytropic region in our temperature distribution beyond a

radius of $\sim 20'$ (Fig. 12) is a relic of this primordial component. Further studies must await future observations with more sensitive X-ray spectrometers and imaging detectors.

We would like to thank the numerous scientists who built, launched, and operated *EXOSAT*. Software from the Institute of Astronomy (XANADU) and the University of Leicester (DGS) was critical in the analysis of our data. We thank the various authors of these software packages and K. Arnaud, R. Shafer, and M. Watson in particular. We would also like to acknowledge Frank Abramopoulos, who supplied us with his computer code for the iron settling problem. This work was supported by NASA grant NSG 5138 and Smithsonian Institution funds.

REFERENCES

Abramopoulos, F., Chanan, G. A., and Ku, W. H.-M. 1981, *Ap. J.*, **248**, 429 (ACK).
Allen, C. W. 1973, *Astrophysical Quantities* (London: Athlone Press), p. 31.
Avni, Y. 1976, *Ap. J.*, **210**, 642.
Bahcall, J. N., and Sarazin, C. L. 1978, *Ap. J.*, **219**, 781.
Bevington, P. R. 1969, *Data Reduction and Error Analysis for the Physical Sciences* (New York: McGraw-Hill), p. 200.
Cavaliere, A., and Fusco-Femiano, R. 1976, *Astr. Ap.*, **49**, 137.
———. 1978, *Astr. Ap.*, **70**, 677.
Chanan, G. A., and Abramopoulos, F. 1984, *Ap. J.*, **287**, 89.
De Young, D. S. 1978, *Ap. J.*, **223**, 47.
Edge, A. C., Stewart, G. C., and Smith, A. 1986, in *NRAO Green Bank Workshop No. 16, Radio Continuum Processes in Clusters of Galaxies*, ed. C. P. O'Dey and J. M. Uson, p. 105.
Fabian, A. C., Nulsen, P. E. J., and Canizares, C. R. 1984, *Nature*, **310**, 733.
Giacconi, R., *et al.* 1979, *Ap. J.*, **230**, 540.
Gioia, I. M., Maccacaro, T., Schild, R. E., Stocke, J. T., Liebert, J. W., Danziger, I. J., Kunth, D., and Lub, J. 1984, *Ap. J.*, **283**, 495.
Gorenstein, P., Fabricant, D., Topka, K., and Harden, F. R., Jr. 1979, *Ap. J.*, **230**, 26.
Gorenstein, P., Fabricant, D., Topka, K., Harnden, F. R., Jr., and Tucker, W. H. 1978, *Ap. J.*, **224**, 718.
Henriksen, M. J., and Mushotzky, R. F. 1986, *Ap. J.*, **302**, 287.
Hughes, J. P. 1988, *Ap. J.*, submitted.
Hughes, J. P., Yamashita, K., Okumura, Y., Tsunemi, H., and Matsuoka, M. 1988, *Ap. J.*, **327**, 615.
Kent, S. M., and Gunn, J. E. 1982, *A.J.*, **87**, 945.
Koyama, K., *et al.* 1984, *Pub. Astr. Soc. Japan*, **36**, 659.
Lampton, M., Margon, B., and Bowyer, S. 1976, *Ap. J.*, **208**, 177.
Merritt, D. 1987, *Ap. J.*, **313**, 121.
Mushotzky, R. F. 1984, *Adv. Space Res.*, **3**, 157.
Mushotzky, R. F., Serlemitsos, P. J., Smith, B. W., Boldt, E. A., and Holt, S. S. 1978, *Ap. J.*, **225**, 21.
Okumura, Y., Tsunemi, H., Yamashita, K., Matsuoka, M., Koyama, K., Hayakawa, S., Masai, K., and Hughes, J. P. 1987, *Pub. Astr. Soc. Japan*, submitted.
Raymond, J. C., and Smith, B. W. 1977, *Ap. J. Suppl.*, **35**, 419.
Rephaeli, Y. 1978, *Ap. J.*, **225**, 335.
Sarazin, C. L., and Bahcall, J. N. 1977, *Ap. J. Suppl.*, **34**, 451.
Sarazin, C. L., Rood, H. J., and Struble, M. F. 1982, *Astr. Ap.*, **108**, L7.
Schattenburg, M. L., and Canizares, C. R. 1986, *Ap. J.*, **301**, 759.
Smith, A., and Stewart, G. C. 1985, in *ESO Workshop on the Virgo Cluster of Galaxies*, ed. O.-G. Richter and B. Binggeli, p. 345.
Taylor, B. G., Andresen, R. D., Peacock, A., and Zobl, R. 1981, *Space Sci. Rev.*, **36**, 641.
The, L. S., and White, S. D. M. 1986, *A.J.*, **92**, 1248.
Toor, A., and Seward, F. D. 1974, *A.J.*, **79**, 995.
Turner, M. J. L., Smith, A., and Zimmermann, H. U. 1981, *Space Sci. Rev.*, **30**, 513.
Ulmer, M. P., Cruddace, R. G., Fenimore, E. E., Fritz, G. G., and Snyder, W. A. 1987, *Ap. J.*, **319**, 118.

D. FABRICANT, P. GORENSTEIN, and JOHN P. HUGHES: Harvard-Smithsonian Center for Astrophysics, 60 Garden Street, Cambridge, MA 02138